Anuário do Instituto de Geociências
Universidade Federal do Rio de Janeiro
https://revistas.ufrj.br/index.php/aigeo/

ISSN 0101-9759
e-ISSN 1982-3908

Mineralogical Characterization of Pegmatites with Occurrences of Halloysite in the Regions of Porciúncula (RJ) and Patrocínio do Muriaé (MG), Southeastern Brazil

Caracterização Mineralógica de Pegmatitos com Ocorrência de Halloysita nas Regiões de Porciúncula – RJ e Patrocínio do Muriaé – MG, Sudeste Brasileiro

Ernesto Adler Licursi[1], Luiz Carlos Bertolino[1] & Francisco José da Silva[2]

[1]Universidade do Estado do Rio de Janeiro, Faculdade de Geologia, Departamento de Mineralogia e Petrologia Ígnea, Rio de Janeiro, RJ, Brasil
[2]Universidade Federal Rural do Rio de Janeiro, Instituto de Agronomia, Departamento de Petrologia e Geotectônica, Rio de Janeiro, RJ, Brasil
E-mails: ernesto.adler@outlook.com; lcbertolino@cetem.gov.br; fjosilva@ufrrj.br
Corresponding author: Ernesto Adler Licursi; ernesto.adler@outlook.com

Abstract

Halloysite ($Al_2Si_2O_5(OH)_4.2H_2O$) is a polymorphic kaolinite mineral whose predominant morphology is tubular. Due to this characteristic, halloysite is widely used in industrial applications, such as manufacture of silica-aluminous catalysts, used for industrial chemical reactions; French porcelain; and the cracking of petroleum fractions into gasoline. Halloysite also has potential as a nanomaterial, particularly as an ingredient in polymer nanocomposites and as active agent for medical, agricultural, and other uses. This clay mineral occurs in a wide variety of geological environments as a product of alteration of rocks rich in sodium and potassium feldspars, such as intrusive acid rocks, granites, anorthosites, and pegmatites. This article characterizes halloysite and describes the treating process of kaolin-halloysite samples from four pegmatites, located in Porciúncula (Rio de Janeiro State) and Patrocínio do Muriaé (Minas Gerais State). The samples of the studied pegmatites were treated for mineralogical characterization and analyzed by X-ray diffractometry and scanning electron microscopy. Density, granulometry, and visual appearance of the grains were also analyzed. The samples were found to be composed of kaolinite/halloysite, feldspar, quartz, biotite, goethite and muscovite. Using X-ray diffractometry, gibbsite were also identified in one sample. With the results presented here, the two regions can be possible targets for researching halloysite deposits in the states of Rio de Janeiro and Minas Gerais.

Keywords: Clay minerals; Nanotechnology; Applied mineralogy

Resumo

A halloysita ($Al_2Si_2O_5(OH)_4.2H_2O$) é um mineral polimorfo da caulinita cuja morfologia predominante é tubular. Devido a essa característica, a halloysita é amplamente usada em aplicações industriais, como na fabricação de catalisadores sílico aluminosos; usada para reações químicas industriais; em porcelanas francesas e no craqueamento de frações de petróleo em gasolina. A halloysita também tem potencial como nanomaterial, particularmente como ingrediente em nanocompostos de polímeros e agentes ativos para medicina, agricultura e outros usos. O argilomineral pode ocorre numa grande variedade de ambientes geológicos como produto de alteração de rochas ricas em feldspatos sódicos e potássicos como rochas ácidas intrusivas, granitos, anortositos e pegmatitos. Esse artigo caracteriza a halloysita e descreve o processo de tratamento de amostras de caulim halloysítico de quatro pegmatitos localizados em Porcíuncula (estado do Rio de Janeiro) e Patrocínio do Muriaé (estado de Minas Gerais). As amostras dos pegmatitos estudados foram beneficiadas para caracterização mineralógica e analisadas por difratometria de raios X e microscopia eletrônica de varredura. Também foram feitas análises de densidade, granulometria e inspeção visual dos grãos. As amostras são constituídas por caulinita/halloysita, feldspato, quartzo, biotita, goethita e muscovita. A gibbsita foi identificada em uma amostra através de difratometria de raios X. Com os resultados apresentados, as duas regiões estudadas podem ser possíveis alvos para pesquisa de depósitos de halloysita nos estados do Rio de Janeiro e de Minas Gerais.

Palavras-chave: Argilominerais; Nanotecnologia; Mineralogia aplicada

Received: 16 May 2022; Accepted: 13 February 2023

1 Introduction

Halloysite and metahalloysite are polymorphic varieties of kaolinite. The characteristic that distinguishes halloysite as a distict kaolin mineral is the presence of molecules of H_2O in the interlayer space (Churchman & Carr 1975). Halloysite morphology is predominantly tubular, but can also be spherical, placoid, or irregular (Joussein et al. 2005), while kaolinite occurs in a hexagonal or pseudo-hexagonal placoid form (Murray 2000). More than one type of halloysite morphology can occur in the same deposit (Pasbakhsh & Churchman 2015). This tubular shape is due to the arrangement of water molecules, interspersed repeatedly every two lamellae (Levis & Deasy 2002). Halloysite occurs in two forms: a hydrated one, with a layer of water molecules between the mineral layers, and a dehydrated one. The hydrated form has basal spacing of 10 Å ($Al_2Si_2O_5(OH)_4.2H_2O$), while the dehydrated form has spacing of 7 Å ($Al_2Si_2O_5(OH)_4$) (Souza Santos, Toledo & Souza Santos 2009).

Since 2007, interest in the potential of halloysite as a nanomaterial, particularly in polymer nanocomposites and active agents for medicine, agriculture, and other uses is rising because of its tubular morphology (Pasbakhsh & Churchman 2015).

The nanometric thickness of the layers can be chemically modified to be compatible with organic polymers. The idea of using halloysite nanotubes in applications is to fill the inner orifice of the tube with the chemical compound of interest and release it in a slow or controlled manner. Studies have been performed to investigate the use of nanotubes in anti-fungicides, paints for walls, antimicrobial compounds, food preservatives and packaging materials, and biomedical applications for the controlled release of drugs (Souza Santos, Toledo & Souza Santos 2009).

Tubular halloysite deposits are generally associated to kaolins formed by weathering or hidrotermalism, being rarely found in deposits of sedimentary kaolin origin. The main deposits in the world are in the state of Utah, USA (Wilson & Keeling 2016), Guizhou, Yunnan and Hunan, China (Wilson 2004), Biga, Turkey (Ece et al. 2008), and the Karikeri-Matauri basin, New Zeeland (Brathwaite et al. 2012).

The kaolin deposits where halloysite occurs in Brazil are located in the South and Southeast regions (Figure 1), mainly in the state of Minas Gerais (Campos & Souza Santos 1986; Pimentel 1966; Souza Santos, Brindley & Souza Santos 1964; Souza Santos, Toledo & Souza Santos 2009; Tolentino Jr. 2019; Wilson, Souza Santos & Souza

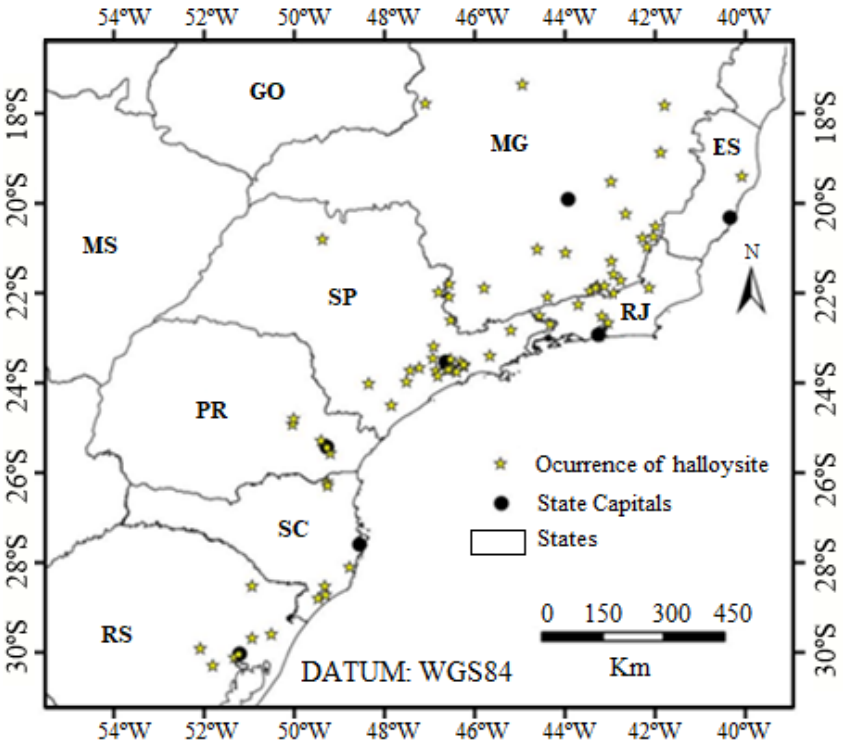

Figure 1 Compilation of pegmatite deposits with halloysite occurrences in the South and Southeast regions of Brazil. Modified from Salgado Campos 2020.

Santos 2006), São Paulo (Angeleri, Souza Santos & Souza Santos 1963; Campos & Souza Santos 1986; Paiva 1956; Pimentel 1966; Souza Santos & Souza Santos 2006; Souza Santos, Toledo & Souza Santos 2009; Visconti & Nicot 1956; Wilson, Souza Santos & Souza Santos 1998) and Rio de Janeiro (Salgado Campos 2020; Santos 2017; Souza Santos, Souza Santos & Moniz 1962; Visconti & Nicot 1957; Visconti & Nicot, 1956).

Recent research carried out by Tolentino Jr. (2019), Salgado Campos (2020) and Salgado Campos et al. (2021) indicates that in the northwest part of the state of Rio de Janeiro, there are pegmatites rich in halloysitic kaolin. However, these occurrences have been poorly studied.

2 Geological Context

The central portion of the Ribeira belt is divided into four different domains: Terreno Ocidental terrain, Paraíba do Sul Klippe, Oriental terrain and Cabo Frio terrain. All pegmatites are inserted in the geological context of Ocidental terrain. A subdivision of three major lithological groups is adopted: 1) Juiz de Fora complex, which has a Paleoproterozoic age of 1.7 Ga and constitutes the basement of the Ocidental terrain (Duarte, Heilbron & Campos-Neto 2000); 2) Andrelândia Megasequence that represents the metasedimentary cover with deposition age ranging from 1.0 to 0.79 Ga (Valeriano et al 2003) and 3) Neoproterozoic granitoids – Pangarito pluton which form a large ellipsoid about 30 km long by 10 km wide, displaying a preferred NE-SW direction (Noce et al 2003).

All pegmatites studied are originated by weathering and located in two distinct areas. The first area (Figure 2A) is located in the northern region of Rio de Janeiro, near the city of Porciúncula. The second area (Figure 2B) is located in the southeastern region of Minas Gerais, near the city of Patrocínio do Muriaé. The pegmatites of Porciúncula are in the geological context of the Andrelândia Megasequence cover, while the pegmatites of Patrocínio do Muriaé are in the geological context of the Neoproterozoic granitoids related to the Pangarito pluton.

3 Materials and Methods

A total of four samples of four pegmatites were collected, one sample per pegmatite, two samples each from Porciúncula (RJ) and Patrocínio de Muriaé (MG). All samples were collected in a punctual-composed manner to represent the pegmatite, and properly sealed to preserve the material. A composite of chip samples, collected in a significant part of each pegmatite or tailings, was obtained to represent the mineralization. That approach was applied to all pegmatite occurrences, to obtain raw samples weighting about 10 kg each.

Initially, the samples were spread out for a period of three days to dry. Then the samples were weighed and comminuted using a jaw crusher adjusted to 2 mm. Next, each sample was homogenized using the conical and longitudinal cell methods. Following that, the samples were separated into aliquots of approximately 1 kg each. Of these aliquots, two were separated to continue the sample treatment procedure and the others were stored. Of these two separate aliquots, one of them was used in the wet granulometric separation with the aid of a vibrating tower. The samples were then separated according to the granulometry and subsequently weighed. Based on the resulting values, granulometric diagrams were generated.

All samples were disaggregated and passed through 106 μm sieves and homogenized. However, this process was carried out in smaller quantities. The samples were separated into smaller aliquots according the purpose, with the objective of obtaining sufficient quantities to be analyzed by each characterization method.

The samples were analyzed by X-ray diffractometry (XRD), using the powder method, performed with a Bruker-AXS D8 Advanced Eco diffractometer, with Cu Kα radiation (40 kV/25 mA), 0.02° 2θ step, count time of 0.52 seconds per step, coupled to a LynxEye XE silicon drift (with energy discrimination), collected from 4 to 70° 2θ. Qualitative spectrum interpretation was performed by comparison with standards contained in the relational database PDF 4+ (ICDD 2014), in the Bruker Diffrac.EVA software. The total acquisition time for each spectrum was approximately 30 minutes.

Scanning electron microscopy (SEM) was performed to obtain high-resolution images of the topographic surface of the studied samples, using a Hitachi model TM3030plus Tabletop Microscope. The samples were coated with silver.

The crystallinity indices of the kaolinites regarding the pegmatites studied were determined by the method proposed by Hinckley (1962).

A stereoscopic microscope was used to observe the characteristics of the mineral grains found in the studied pegmatites. The magnification of the grains allowed the visual mineralogical characterization of the samples.

The brightness index was measured using a Technidyne ISO colorimeter. The procedure was to weigh 5 grams of a completely dry sample, place the sample in a cylinder to compact the material, and finally take the reading.

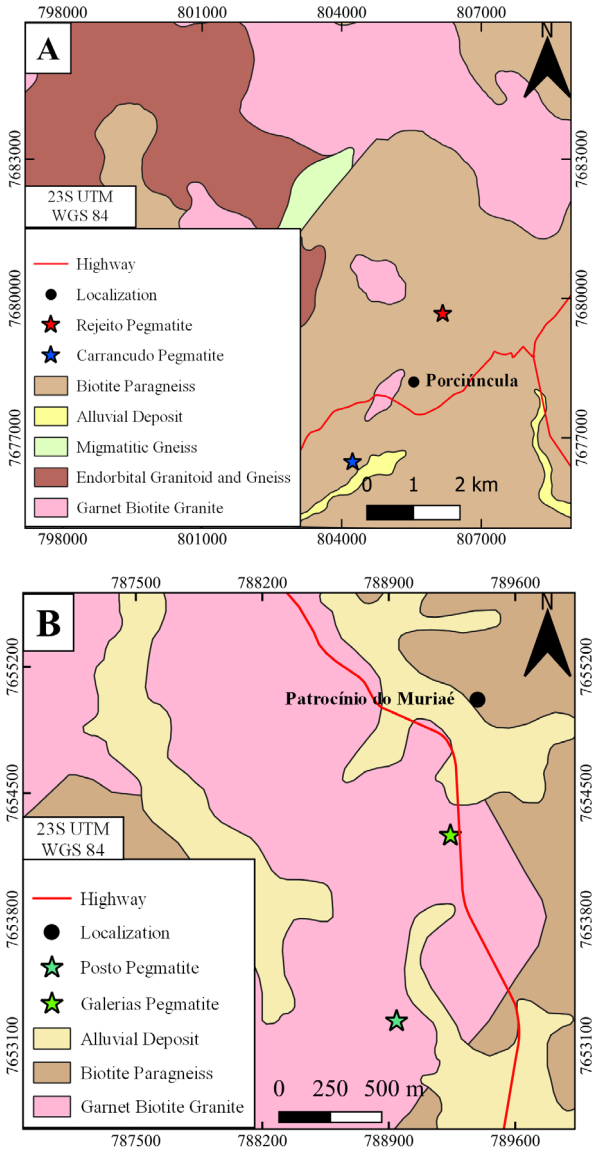

Figure 2 A. Lithostratigraphic map of a region near Porciúncula showing the location of Rejeito pegmatite and Carrancudo pegmatite (modified from Noce et al. 2012); B. Lithostratigraphic map of a region near Patrocínio do Muriaé showing the location of Posto pegmatite and Galerias pegmatite (modified from Romano & Noce 2003).

4 Results

4.1 Fieldwork

Sampling was conducted to obtain altered material from pegmatites for laboratory mineralogical characterization in order to identify halloysite.

Rejeito pegmatite sample (Figure 3A), collected at the coordinates 806170E 7679674N, is inserted in the geological context of Andrelândia Unit. It was possible to observe vestiges of old workings, which are now silted up, with only a few tailings mounds found in the area. The tailings are mostly altered, with whitish color, containing subhedral quartz crystals ranging from fine to coarse, subhedral grains of centimetric to decimetric muscovite, subhedral feldspar grains with fine to coarse granulometry, and kaolin.

Carrancudo pegmatite sample (Figure 3B) was obtained at coordinates 804232E 7676482N, also inserted in the geological context of the Andrelândia Unit. It has a light color, shows an intense alteration process and is basically composed of kaolin, subhedral muscovite grains, subhedral feldspar and subhedral quartz. It is hosted in a weathered orthogneiss in an outcrop having approximate dimensions of 8 meters high by 6 meters wide.

Posto pegmatite sample (Figure 3C) occurs at the coordinates 788944E 7653237N and is inserted in the geological context of the Pangarito pluton. It is mostly weathered and the outcrop has approximate dimensions of 8 meters high by 50 meters wide. The main minerals consist of grains of kaolin, subhedral quartz ranging from fine to coarse, grains of subhedral feldspar ranging from fine to coarse, and grains of subhedral muscovite ranging from fine to medium. It is hosted in a weathered granite-gneiss unit cut by feldspathic quartz apophyses.

Galerias pegmatite sample (Figure 3D) occurs at the coordinates 789242E 7654266N and is also inserted in the geological context of the Pangarito pluton. It is located in tailings mounds with an approximate height of 3 meters. The tailings contain kaolin, subhedral muscovite grains, subhedral quartz with granulometry varying from fine to medium, feldspar grains ranging from fine to medium and subhedral to centimetric tourmaline grains, with approximately 4 centimeters. The color of the tailings is reddish-white.

4.2 Granulometric Classification

A wet granulometric classification was performed, using a vibrating tower. In total, 14 sieves were used. The last sieve was 44 μm. The grains that passed throught the 44 μm were used for the methods of X- ray diffractometry, scanning eletron microscopy, magnetic separation and brightness index. Separating the samples into different fractions helps the process of identification of clays minerals, as they have a low granulometry and are concentrated in fractions bellow 44 μm.

The graphs show similarity between the linear behavior of the samples of Rejeito pegmatite (Figure 4A), Carrancudo pegmatite (Figure 4B) and Galerias pegmatite (Figure 4D), with very similar values of both pass-through and acumulated mass. The graph referring to Posto pegmatite (Figure 4C) exhibits a slightly different behavior, with almost 50% of the grains being smaller than 44 μm**.**

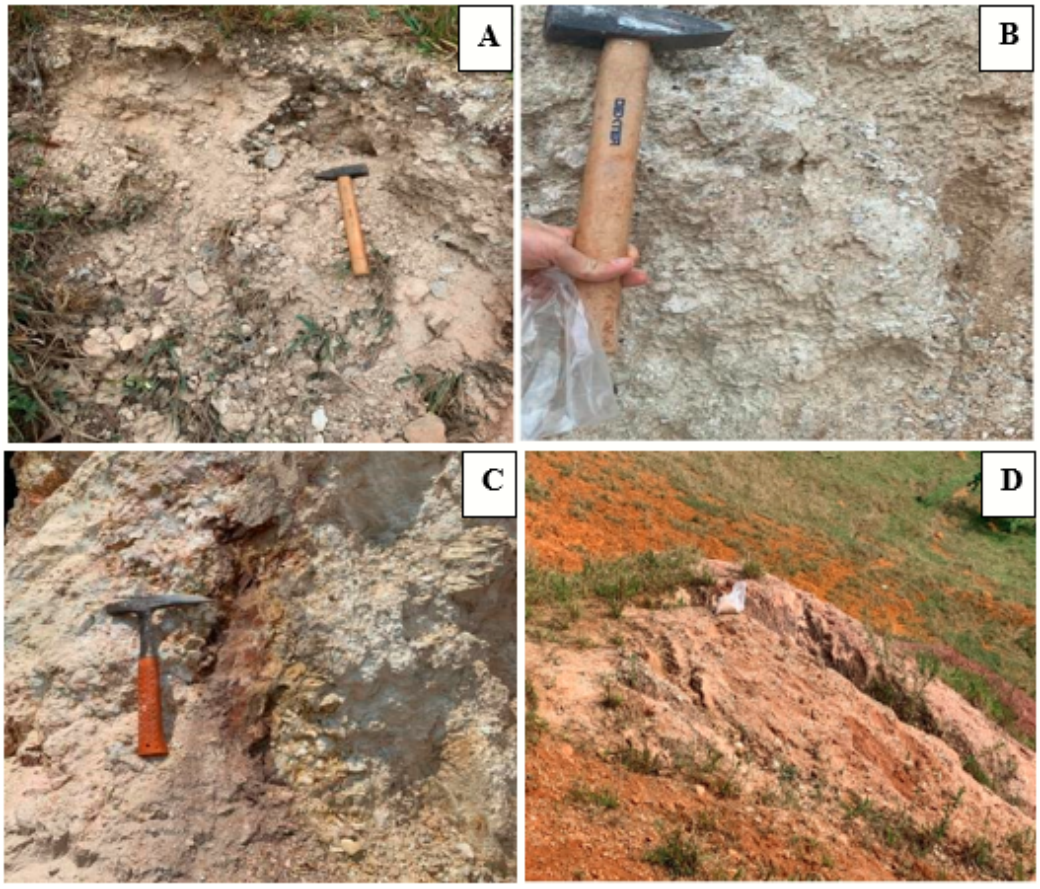

Figure 3 Photographs of studied pegmatites: A. Image of Rejeito pegmatite showing tailings where the samples were obtained; B. Carrancudo pegmatite sampling site with the occurrence of kaolin; C. Detail of the sampling site showing the occurrence of kaolin in Posto pegmatite; D. View of Galerias pegmatite depicting old workings.

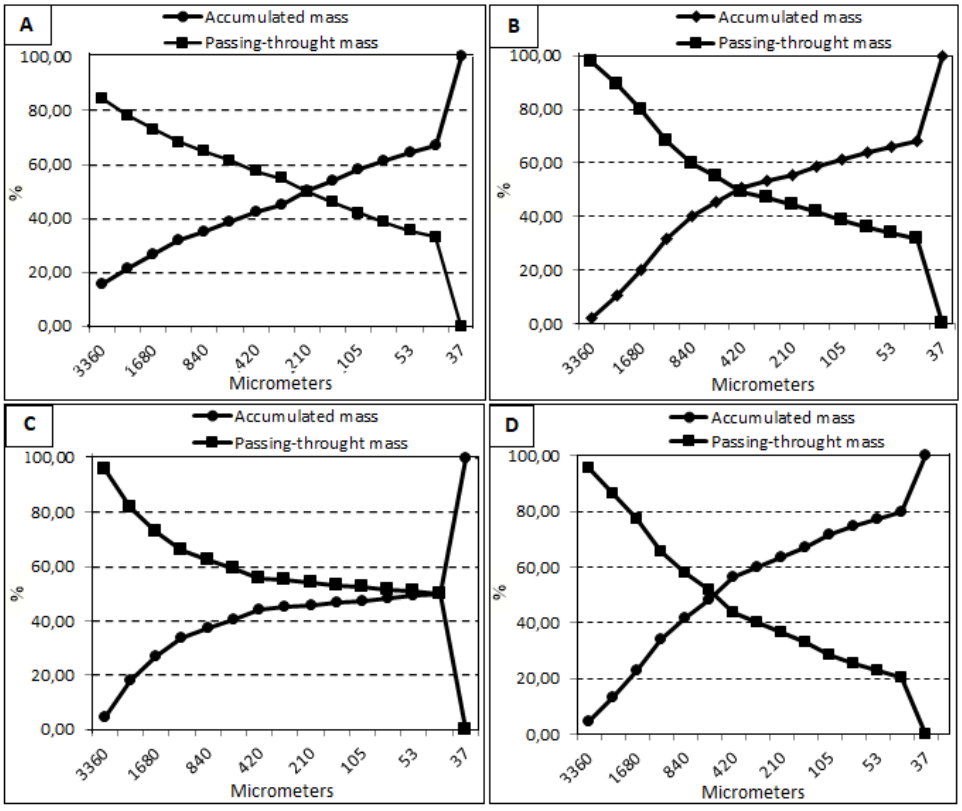

Figure 4 Granulometric distribution of samples of: A. Rejeito pegmatite; B. Carrancudo pegmatite; C. Posto pegmatite; D. Galerias pegmatite.

4.3 Stereo Microscopy

Stereo microscopy was used to inspect the coarser grains of the studied pegmatite samples. The observation of kaolin is difficult due to its low granulometry, usually concentrated in <44 mm fractions.

Figure 5 shows the grains of Rejeito, Carrancudo, Posto and Galerias Pegmatites, where it is possible to identify the presence of: quartz (Qz) and feldspar (Fsp), which constitute approximately 90% of the grains, while the other 10% are constituted by accessory minerals such as muscovite (Ms) and biotite (Bt), composing the total sample. Quartz and feldspar grains are angular with a glassy shine while mica grains have a lamellar arrangement and a micaceous sheen. The grain size fractions observed are below 6 mm and below 2 mm.

4.4 X-ray Diffractometry

X-ray diffractograms were obtained from 16 samples of the four studied pegmatites. For each sample (peg), four fractions were selected and analyzed: crude fraction, magnetic fraction < 44 μm, non-magnetic fraction < 44 μm, and fraction < 44 μm. Figure 6 shows the diffractograms related to these samples, where mica of 10 Å halloysite/kaolinite of 7 Å, K-feldspar of 3.8 Å and 3.2 Å, quartz of 3.3 Å and 4.2 Å, gibbsite of 5 Å and goethite of 2.4 Å are identified.

In the < 44 μm fraction's diffractograms, an increase in kaolinite intensity and a decrease in quartz can be observed. The opposite happens with the crude fraction. This happens because kaolinite is concentrated in the finest fractions.

4.5 Hinckley Crystallinity Index

The Hinckley crystallinity index was created to measure the crystallinity degree of kaolinite, aiming to estimate the ordering degree. Kaolinites from Rejeito pegmatite to Galerias pegmatite present indices of 0.70, 0.26, 1.09 and 0.56, respectively (Table 1).

4.6 Scanning Electron Microscopy

Scanning electron microscopic images were obtained to differentiate kaolinite from halloysite in the clay fractions of the pegmatites. Mixed images (backscattered electronic image (BSE) superimposed on secondary electron image (SE) are shown.

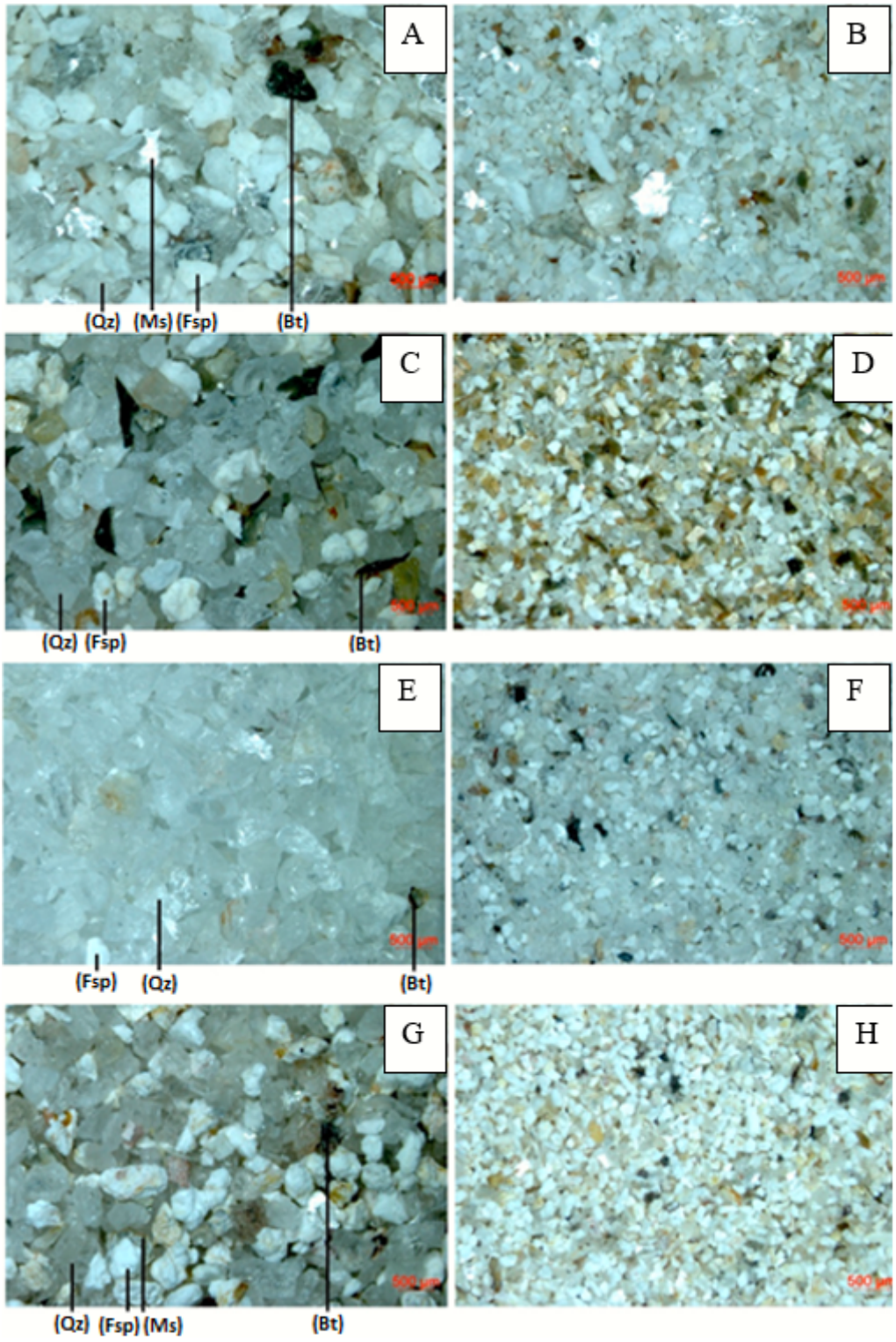

Figure 5 Photograph of the grains: A, C, E, G. Grains of Rejeito, Carrancudo, Posto and Galerias Pegmatites, respectively, under 6 mm; B, D, F, H. Grains of Rejeito, Carrancudo, Posto and Galerias Pegmatites, respectively, under 2 mm; Qz = Quartz, Fsp = Feldspar, Ms = Muscovite. Bt = Biotite.

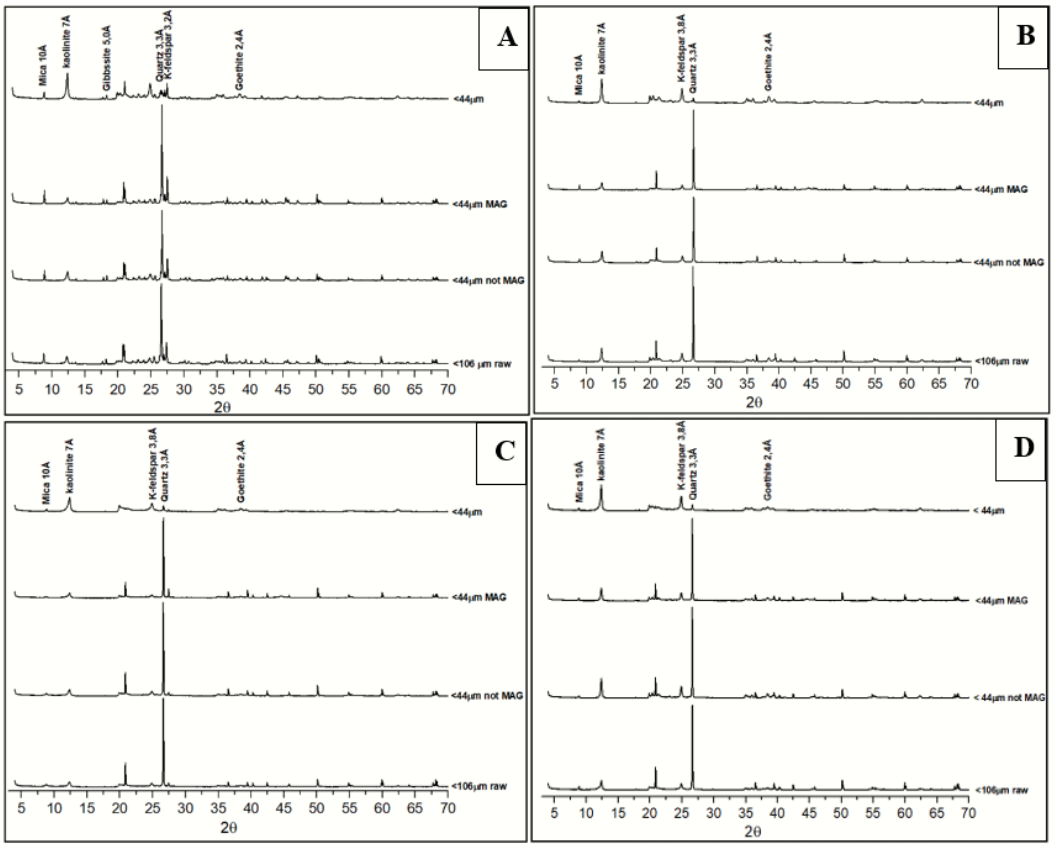

Figure 6 X-Ray diffractograms of samples of: A. Rejeito pegmatite; B. Carrancudo pegmatite; C. Posto pegmatite; D. Galerias pegmatite.

Table 1 Hinckley crystallinity indices of the kaolinite from the studied pegmatites.

Pegmatite	H	B	H + B	Ht	HI
Rejeito pegmatite	0.56	0.64	1.21	1.72	0.70
Carrancudo pegmatite	0.39	0.34	0.73	2.76	0.26
Posto pegmatite	1.55	1.30	2.85	2.62	1.09
Galerias pegmatite	0.51	0.45	0.96	1.72	0.56

The image of the sample of Rejeito pegmatite shows the occurrence of halloysite in tubular form. In the image that shows the crude fractions of Rejeito pegmatite (Figure 7A), it is possible to see the slightly altered kaolinite grains in booklet form. Halloysite tubes have length up to 3 µm. In the < 44 µm fraction (Figure 7B), it is possible to see that the halloysite tubes grow on feldspar grains.

In the images of the samples of Carrancudo pegmatite, there are abundant tubular crystals of halloysite. Halloysite can be observed in the crude fraction (Figure 7C) growing over a feldspar grain, exhibiting a rich clay mineral surface. In the < 44 µm fractions (Figure 7D), it is possible to see not only tubular halloysite grains, but also feldspar grains exceeding 40 µm.

Unlike the other pegmatite samples, halloysite was not found in Posto pegmatite. The feldspar is altered by the weathering process in the crude fraction (Figure 7E). In the < 44 µm fraction (Figure 7F), there is abundant kaolinite with pseudo-hexagonal habit forming booklets reaching up to 40 µm. This well-formed kaolinite indicates that the mineral was formed in situ. This sample presents the highest crystallinity index, reflecting its well-formed grains.

In the images of the samples of Galerias pegmatite, it is possible to see halloysite and kaolinite coexisting. Halloysite appears with tubular morphology reaching 3 µm (Figure 8A). The halloysite grows not only on the feldspar grains but also in kaolinite grains (Figure 8B).

4.7 Brightness Index

The brightness index results that were generated refer to the non-magnetic particle size fraction < 44 µm of all studied pegmatites. The values range from 51.52 to 68.98 (ISO % – International Organization of Standardization – Brightness index) (Figure 9).

The highest value is related to the sample of Galerias pegmatite and the lowest value is related to the sample of Posto pegmatite.

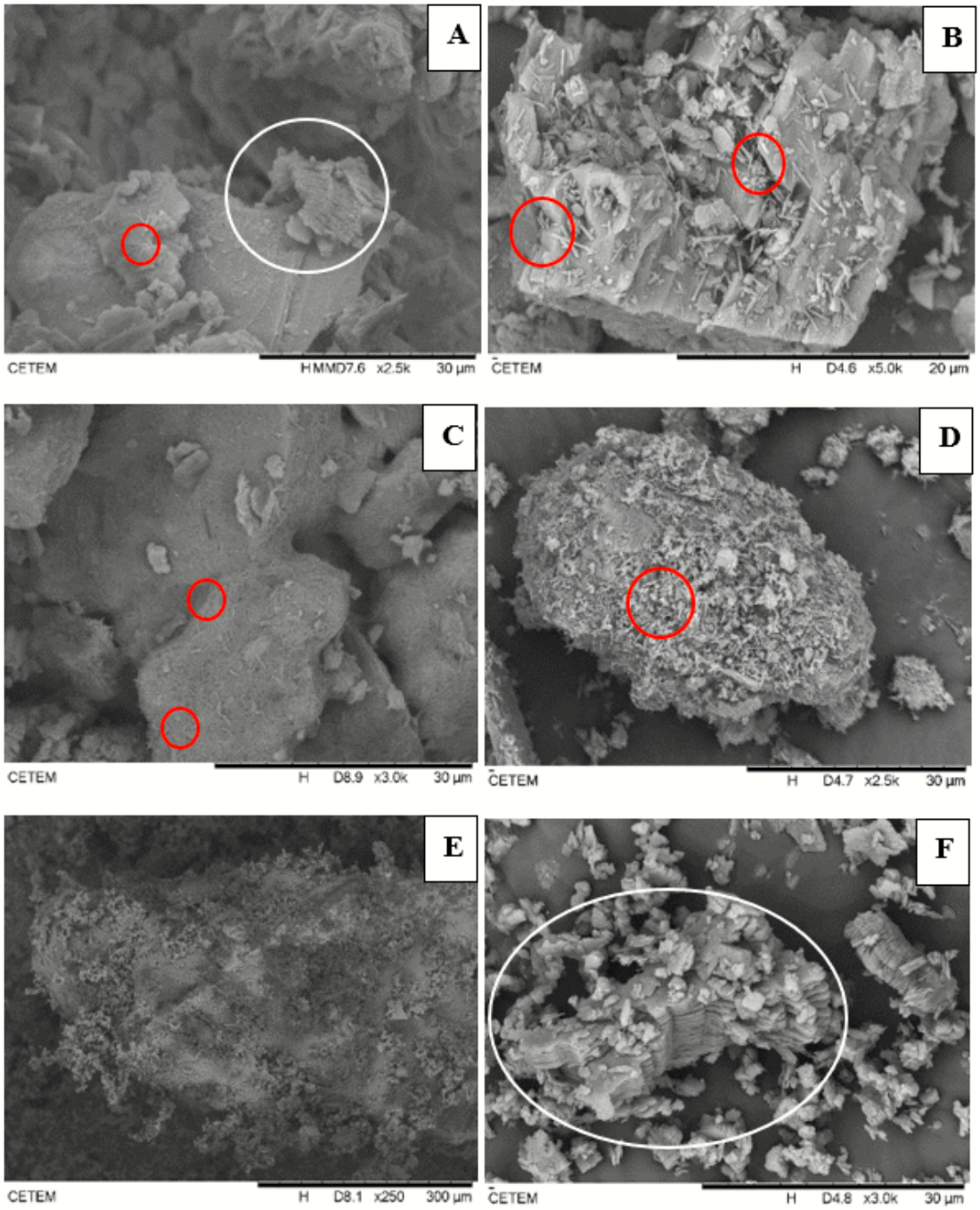

Figure 7 Backscattered SEM Images of the grains of the studied pegmatites: A-B. Presence of tubular halloysite and booklets of kaolinite in the Rejeito pegmatite raw sample and < 44 µm fraction, respectively; C-D. Presence of abundant tubular halloysite in the Carrancudo pegmatite samples; E. Grain of feldspar showing irregular surface produced by weathering of the Posto pegmatite raw sample; F. Presence of hexagonal kaolinite in Posto pegmatite.

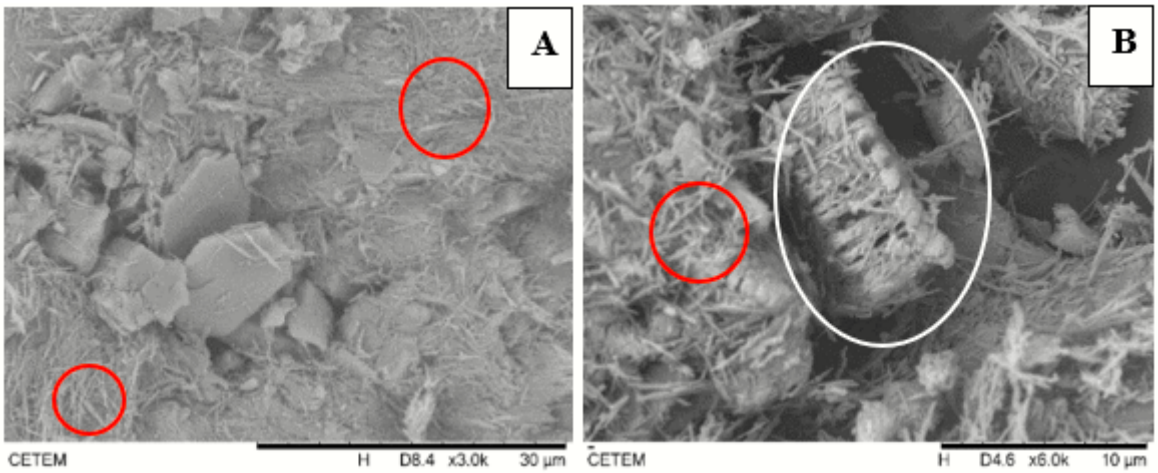

Figure 8 Backscattered SEM Images of the grains of the studied pegmatites: A-B. Presence of abundant tubular halloysite growing over the kaolinite in both samples of Galerias pegmatite.

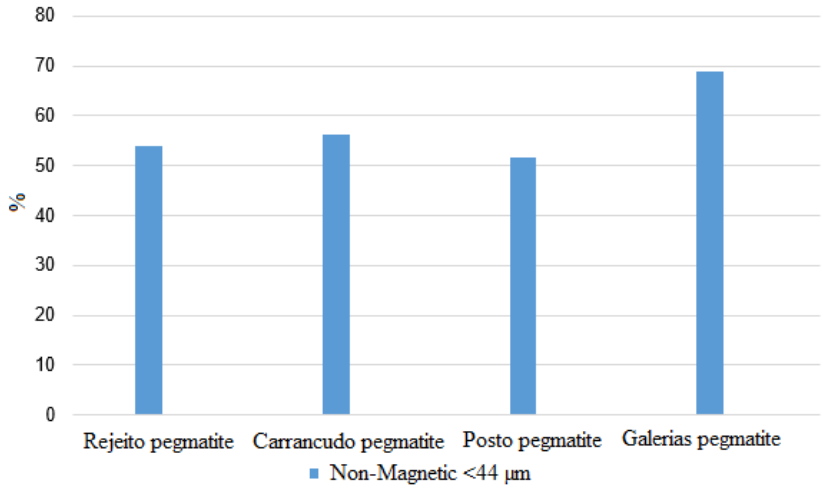

Figure 9 Comparison showing the brightness indices obtained for the samples from the studied pegmatites.

5 Discussion

We could not observe structural features in the studied outcrops due to deep weathering or lack of geological context in the case of material originated from old workings.

The pegmatites are located in a tropical region characterized by seasonal high temperatures and heavy rainfall, conducive to the formation of halloysite in weathered granites and pegmatites (Bristow 1987). Occurrences of the mineral in nearby regions have been identified (Tolentino Jr. 2019; Salgado Campos 2020).

The mineral assemblage of the thickest fractions of the studied rocks is basically composed of quartz, feldspar, biotite and muscovite, while kaolin only appears in the finer fractions. Posto pegmatite is low in feldspar and mica, composed almost by quartz grains. This added to the fact that the percentage of passing mass through the sieves of grains below 44 µm (49.82 %) (6.05%) indicates that Posto pegmatite suffered the most severe weathering process.

The values from X-ray diffractograms for crystallinity indices of kaolinite are in the range of 0.26-1.09. Posto pegmatite contains kaolinite with the highest Hinckley index, indicating crystals with greater ordering. This value is reflected in better crystallized grains, as observed in the SEM images.

The brightness indexes (51.52 to 68.98 (%ISO)) are relatively low for the paper industry. These low values are probably due to fewer impurities, such as iron and titanium which when oxidized make the kaolin redder, when whiteness is desired (Gonçalves, Petter & Machado 2012).

SEM images shows altered feldspar grains in < 44 µm and raw fractions. Halloysite tubes and kaolinite

booklets were found not only in the feldspar surface, but also in interstices. It suggests that there is a genetic correlation between the weathering process of felpdspar and the formation of halloysite tubes from the recrystallization of this grains. The images shows that when the halloysite occurs on the surface of unformed kaolin, the halloysite appears in abundance, while when the kaolinites are well formed, the halloysite is restricted. When the pegmatite is very weathered, halloysite does not appear in large quantities, but the amount of kaolinite is high. This recrystallization from halloysite to kaolinite occurs when weathering levels are high (Papoulis, Katagas & Katagas 2004). This is probably because in this process there is a loss of water molecules from the halloysite tubes and this loss makes the oxygen atoms on the surface of the tetrahedral sheet stretch the basal hydroxyl groups of the adjacent octahedral sheet, making halloysite lose its shape, "unrolling" and then forming kaolinite plates (Bates 1959). Since one of the factors controlling the formation of halloysite is the feldspar's level of weathering, it is suggested that there is a specific interval of appearance of halloysite for its formation and preservation.

According to Papoulis, Katagas & Katagas (2004), in their analysis of weathered gneiss profiles, kaolinite predominates in more weathered rocks than halloysite, which is more common near fresh gneisses. Since Posto pegmatite is the most weathered body analyzed and the only pegmatite solely containing kaolinite, the observation of the mentioned author coincides with the results of the present study.

6 Conclusion

The studied area is favorable for the deposits of halloysite, as observed in the pegmatite bodies.

The mineralogical characterization methods used, namely SEM, XRD, grain inspection using a stereomicroscope and measurements of density and brightness proved to be efficient,

The SEM images were very useful to distinguish halloysite from kaolinite, clearly showing the halloysite tubes and kaolinite booklets. The XRD revealed the mineralogy of the studied pegmatites, including the existence of quartz, k-feldspar, kaolinite/halloysite, gibbsite and goethite.

The studied samples had relatively low brightness values, from 51.52 to 68.98 (%ISO). For use in ceramics and paper industry, the recommended percentages should be around 75-90% and 82-92%, respectively (Prasad, Reid & Murray 1991).

A higher degree of weathering in granite/pegmatite may explain the formation of kaolinite at the expense of halloysite, suggesting the existence of a weathering level gap in which halloysite remains stable before becoming kaolinite (Papoulis, Katagas & Katagas 2004).

The geological features which identify and control the presence of halloysite are still largely unknown, so more research is necessary.

7 Acknowledgments

We thank the Center for Mineral Technology (CETEM/MCTI), the Postgraduate Program in Geosciences of the Rio de Janeiro State University (UERJ), the Carlos Chagas Filho Research Foundation of the State of Rio de Janeiro (FAPERJ) (process 202.120/2020) and the National Council for Scientific and Technological Support (CNPq) for the financial support

8 References

Angeleri, F.B., Souza Santos, P. & Souza Santos, H. 1963, 'Características físico-químicos e cerâmicos de caulins e argilas usados na Indústria Cerâmica de S. Paulo. VII - Caulins creme amarelados de Parelheiros, Estado de S. Paulo', *Cerâmica,* vol. 9, no. 3, pp. 19.

Bates, T.F. 1959, 'Morphology and crystal chemistry of 1:1 layer lattice silicates', *American Mineralogist*, vol. 44, no. 1, pp. 78-114.

Brathwaite, R.L., Christie, A.B., Faure, K., Townsend, M.G. & Terlesk, S. 2012, 'Origin of the Matauri Bay halloysite deposit, Northland, New Zealand', *Mineralium Deposita*, vol. 47, no. 8, pp. 897– 910, DOI:10.1007/s00126-012-0404-9.

Bristow, C.M. 1987, 'World kaolins: Genesis, exploitation and application', *Industrial Minerals*, pp. 45-9.

Campos, T.W. & Souza Santos, H. 1986, 'Estudo de caulins brasileiros por microscopia eletrônica de transmissão', *Cerâmica*, vol. 32, pp. 355-60.

Churchman, G.J. & Carr R.M. 1975, 'The definition and nomenclature of halloysites', *Clays and Clay Minerals*, vol 23, pp. 382-88.

Duarte, B.P., Heilbron, M., Campos-Neto, M.C. 2000, 'Granulite/ charnockite from the Juiz de Flora Domain, Central Segment of Brasiliano Ribeira Belt' *Revista Brasileira de Geociências*, vol. 30, no. 3, pp. 358-62.

Ece, Ö.I., Schroeder, P.A., Smilley, M.J. & Wampler, J.M. 2008, 'Acid-sulphate hydrothermal alteration of andesitic tuffs and genesis of halloysite and alunite deposits in the Biga Peninsula, Turkey', *Clay Minerals*, vol. 43, no. 2, pp. 281–315, DOI:10.1180/claymin.2008.043.2.10.

Gonçalves, Í.G., Petter, C.O. & Machado J.L. 2012, 'Quantification of hematite and goethite concentrations in kaolin using diffuse reflectance spectroscopy: a new approach to Kubelka–Munk theory', *Clays and Clay Minerals*, vol. 60, no. 5, pp. 473–83, DOI:10.1346/CCMN.2012.0600504.

Hinckley, D.N. 1962, 'Variability in "crystallinity" values among the kaolin deposits of the coastal plain of Georgia and South Caroline', *Clays Clay Miner*, no. 11, pp. 229-35.

ICDD - International Centre for Diffraction Data 2014, *PDF4+ version 2014 (Database)*, International Centre for Diffraction Data, Newtown Square.

Joussein, E., Petit, S., Churchman, J., Theng, B., Righi, D. & Delvaux, B. 2005, 'Halloysite clay minerals - a review', *Clay Minerals*, vol. 40, no. 4, pp. 383–426, DOI:10.1180/0009855054040180.

Levis, S.R & Deasy, P.B. 2002, 'Characterization of halloysite for use as a microtubular drug delivery system', *International Journal of Pharmaceutics'*, vol. 243, no. 1-2, pp. 125-34, DOI:10.1016/S0378-5173(02)00274-0.

Murray, H.H. 2000, 'Traditional and new applications for kaolin, smectite, and palygorskite: a general overview', *Applied Clay Science*, vol. 17, pp. 207-21, DOI:10.1016/S0169-1317(00)00016-8.

Noce, C.M., Novo, T.A., Figueiredo, C.M., Pedrosa-Soares, A.C. 2012, *Geologia e recursos minerais da folha Carangola SF.23-X-B-VI*, Relatório técnico, Mapa Escala 1:100.00.

Noce, C.M, Romano, A.W, Pinheiro, C.M, Mol, V.S, Pedrosa Soares, A.C. 2003, 'Geologia das Folhas Ubá e Muriaé', in A.C. Pedrosa-Soares, C.M. Noce, R. Trouw & M. Heilbron (coord.), *Projeto Sul de Minas*, vol. 1, COMIG/SEME, Belo Horizonte, pp. 153-258.

Paiva, N.J.E. 1956, 'Características de alguns caulins dos arredores da cidade de São Paulo', *Cerâmica*, vol. 2, pp. 111-44.

Papoulis, D., Katagas, T.P. & Katagas, C. 2004, 'Progressive stages in the formation of kaolin minerals of different morphologies in the weathering of plagioclases', *Clays and Clays Minerals*, vol. 52, no. 3, pp. 275-86, DOI:10.1346/CCMN.2004.0520303.

Pasbakhsh, P. & Churchman, G.J. 2015, *Natural Mineral Nanotubes: Properties and applications*, 1st edn, Apple Academic Press, Oakville.

Pimentel, A.C. 1966, 'Distribuição geográfica de caulins cauliníticos e halloysíticos do Brasil', *Cerâmica*, vol. 12, pp. 161-72.

Prasad, M.S., Reid, K.J. & Murray, H.H. 1991, 'Kaolin: processing, properties and applications', *Applied Clay Science*, vol. 6, no. 2, pp. 87-119, DOI:10.1016/0169-1317(91)90001-P.

Romano, A.W & Noce, C.M. 2003, *Carta Geológica da Folha de Muriaé – Folha SF.23-X-D-III Muriaé*, Escala: 1.100.000.

Salgado Campos, V. 2020, 'Prospecção e Caracterização Mineralógica, química e Micromorfológica de Ocorrências de Caulim da Província Pegmatítica do Rio de Janeiro visando a Identificação de Depósitos de Halloysita', Dissertation, Universidade Federal do Rio de Janeiro.

Salgado Campos, V., Bertolino, L.C., Silva, F.J., Mender, J.C., Neumann, R. 2021, 'Mineralogy and chemistry of a new halloysite deposit from the Rio de Janeiro pegmatite province, south-eastern Brazil', *Clays Mineral*, vol. 56, no. 1, pp. 1-15, DOI:10.1180/clm.2021.8.

Santos, H.A.B.J. 2017, 'Caracterização mineralógica do caulim proveniente de pegmatitos da região de Rio Bonito – RJ visando a identificação de halloysita', PhD Thesis, Universidade Federal Rural do Rio de Janeiro.

Souza Santos, P., Souza Santos, H. & Moniz, A. C. 1962, 'Estudos de algumas argilas e caulins de diversos Estados do Brasil', *Cerâmica,* vol. 8, pp. 2-21.

Souza Santos, P., Brindley. W. & Souza Santos, H. 1964, 'Mineralogical studies of kaolinite-halloysite clays: part II some Brazilian kaolins', *American Mineralogist*, vol. 49, no. 1-2, pp. 1543-8.

Souza Santos, P., Toledo, S.P. & Souza Santos, H. 2009, 'Caulins Haloisíticos das Regiões Sudeste e Sul do Brasil', *Cerâmica Industrial*, vol. 14, no. 1, pp. 14-20.

Tolentino Jr, J. 2019, 'Potencial dos depósitos de caulim halloysítico associados aos pegmatitos da região de Juiz de Fora visando o seu aproveitamento econômico', PhD thesis, Universidade do Estado do Rio de Janeiro.

Valeriano, C.M., Machado, N., Simonetti, A., Valladares, C.S., Seer, H. & Simões, L.S. 2003, 'U-Pb ages of detritial zircons and provenance of Proteroizoic metasedimentary units around southwestern and southern São Francisco craton', *IV South American Symposium on Isotope Geology, Shorts Papers*, vol. 1, pp. 300-3.

Visconti, Y.S. & Nicot, N.B.F. 1956, 'Novas observações relativas aos caulins tubulares por meio de dispersão química e do microscópio eletrônico', *Cerâmica,* vol. 2, no 6, pp. 59-65.

Visconti, Y.S. & Nicot, B.N.F. 1957, 'Mutilização do caulim tubular', *Cerâmica*, vol. 3, no. 10, pp. 72-80.

Wilson, I. & Keeling, J. 2016, 'Global occurrence, geology and characteristics of tubular halloysite deposits', *Clay Minerals*, vol. 51, no. 3, pp. 309-24, DOI:10.1180/claymin.2016.051.3.12.

Wilson, I.R. 2004, 'Kaolin and halloysite deposits of Chine', *Clay Minerals*, vol. 39, no. 1, pp. 1-15, DOI:10.1180/000985543910116.

Wilson, I.R., Souza Santos, H. & Souza Santos, P. 1998, 'Caulins brasileiros: Alguns aspectos da geologia e da mineralogia', *Cerâmica*, vol. 44, no. 287-288, pp. 287-8, DOI:10.1590/S0366-69131998000400003.

Wilson, I.R., Souza Santos, H. & Souza Santos, P. 2006, 'Kaolin and halloysite deposits of Brazil', *Clay Minerals*, vol. 41, no. 3, pp. 697-716, DOI:10.1180/0009855064130213.

Author contributions
Ernesto Adler Licursi: conceptualization; writing – original draft; formal analysis; writing-original draft; visualization. **Luiz Carlos Bertolino:** methodology; conceptualization; supervision; validation; funding acquisition. **Francisco José da Silva:** writing – review and editing; validation; formal analysis; supervision.

Conflict of interest
The authors declare no conflict of interest.

Data availability statement
All data included in this study are publicly available in the literature.

Funding information
FAPERJ, Process Nº E-26/202.120/2020.

How to cite:
Licursi, E.A., Bertolino, L.C. & Silva, F.J. 2023, 'Mineralogical Characterization of Pegmatites with Occurrences of Halloysite in the Regions of Porciúncula (RJ) and Patrocínio do Muriaé (MG), Southeastern Brazil', *Anuário do Instituto de Geociências,* 46:52487. https://doi.org/10.11137/1982-3908_2023_46_52487